Neurosci. Bull. January, 2022, 38(1):69–80
https://doi.org/10.1007/s12264-021-00747-z

www.neurosci.cn
www.springer.com/12264

ORIGINAL ARTICLE

Effect of Sodium Salicylate on Calcium Currents and Exocytosis in Cochlear Inner Hair Cells: Implications for Tinnitus Generation

Ting Fan[1,2] · Meng-Ya Xiang[1,2] · Ruo-Qiao Zhou[1,2] · Wen Li[1,2] · Li-Qin Wang[1] · Peng-Fei Guan[1,2] · Geng-Lin Li[1] · Yun-Feng Wang[1,2] · Jian Li[3]

Received: 4 January 2021 / Accepted: 29 April 2021 / Published online: 7 July 2021

Abstract Sodium salicylate is an anti-inflammatory medication with a side-effect of tinnitus. Here, we used mouse cochlear cultures to explore the effects of salicylate treatment on cochlear inner hair cells (IHCs). We found that IHCs showed significant damage after exposure to a high concentration of salicylate. Whole-cell patch clamp recordings showed that 1–5 mmol/L salicylate did not affect the exocytosis of IHCs, indicating that IHCs are not involved in tinnitus generation by enhancing their neuronal input. Instead, salicylate induced a larger peak amplitude, a more negative half-activation voltage, and a steeper slope factor of Ca^{2+} current. Using noise analysis of Ca^{2+} tail currents and qRT-PCR, we further found that salicylate increased the number of Ca^{2+} channels along with $Ca_V1.3$ expression. All these changes could act synergistically to enhance the Ca^{2+} influx into IHCs. Inhibition of intracellular Ca^{2+} overload significantly attenuated IHC death after 10 mmol/L salicylate treatment. These results implicate a cellular mechanism for tinnitus generation in the peripheral auditory system.

Keywords Salicylate · Tinnitus · Inner hair cell · Calcium current · Exocytosis · Whole-cell patch clamp · $Ca_V1.3$ channel

Introduction

Sodium salicylate, the active ingredient of the commonly used nonsteroidal anti-inflammatory drug aspirin, can induce transient tinnitus in patients during the course of medication [1], and thus has been widely adopted to establish animal models and study the mechanisms of tinnitus [2–5]. Tinnitus is a phantom sensation characterized by hearing sound without corresponding objective external stimulation [6]; it is closely associated with anxiety, depression, and insomnia [7]. The prevalence of tinnitus ranges between 10% and 15% in the adult population [6], and can reach up to 42.7% in the elderly [8]. Although the number of published reports on tinnitus has shown remarkable growth due to the development of functional imaging and electrophysiological techniques, the underlying mechanisms of this disorder remain unclear.

It is widely accepted that changes in spontaneous neural activity in the auditory system play important roles in tinnitus generation. In fact, identifying the neural generator(s) has long been one of the major topics in tinnitus research. Using the whole-cell patch clamp technique, electrophysiological characteristics has been studied in various regions in the auditory pathway under salicylate treatment, including the auditory cortex [3, 9], inferior colliculus [10], dorsal cochlear nucleus [5, 11], spiral ganglion neurons [2, 4, 12, 13], and cochlear hair cells

Ting Fan and Meng-Ya Xiang have contributed equally to this work.

✉ Geng-Lin Li
genglin.li@fdeent.org

✉ Yun-Feng Wang
wyf80612@126.com

✉ Jian Li
lijianjulia@fudan.edu.cn

[1] ENT Institute and Department of Otorhinolaryngology, EYE & ENT Hospital, Fudan University, Shanghai 200031, China

[2] NHC Key Laboratory of Hearing Medicine, Fudan University, Shanghai 200031, China

[3] Clinical Laboratory Center, Children's Hospital of Fudan University, Shanghai 201102, China

[14, 15]. Although numerous animal models of tinnitus have provided evidence for a cortical origin, cochlear hair cells are also considered to play a critical role in its generation. Kakehata and Santos-Sacchi found that salicylate affects the motility and capacitance of cochlear outer hair cells (OHCs) through direct interactions with its sensor/motor [16]. In addition, salicylate directly blocks the K^+ outflow in isolated inner hair cells (IHCs) [14].

However, the effects of salicylate on Ca^{2+} currents and exocytosis in IHCs have not been reported. IHCs are peripheral mechanosensory cells that transform mechanical stimuli into neuronal signals [17]. The exocytosis of IHCs is mediated by inward Ca^{2+} current through the $Ca_V1.3$ type of Ca^{2+} channels [18], constituting the basis of cochlear neural output, and may also be involved in the generation of tinnitus. To fill this knowledge gap, we used cochlear cultures to study the electrophysiological changes of IHCs induced by salicylate, aiming to explore the molecular mechanism for the generation of tinnitus in the peripheral auditory system.

Materials and Methods

Animals

C57BL/6J mice 6 days old (P6) were obtained from the Department of Laboratory Animal Science of Fudan University. After inhalation anesthesia, mice were acutely decapitated with dissecting scissors, and then quickly used for dissection and further experiments. All the experimental procedures were in accordance with the Guide for the Care and Use of Laboratory Animals published by the National Institutes of Health (NIH, USA) and were approved by the Shanghai Medical Experimental Animal Administrative Committee. We have made every effort to keep the number of experimental animals used and their pain to a minimum.

Cochlear Cultures and Drug Administration

The intact sensory epithelia of the cochlea (stria vascularis and spiral ganglion removed) were carefully dissected in pre-cooled phosphate-buffered saline (PBS) and then stuck on coverslips coated with Cell-Tak (BD Biosciences, Franklin Lakes, NJ, USA). We retained the whole sensory epithelia to make it easier to identify the middle turn when performing patch clamp recordings (Fig. 1B). The culture medium and culture conditions were as previously described [19]. After 3-day incubation for stabilization, the explants were randomly divided into blank control and experimental groups treated with different concentrations of sodium salicylate (1 mmol/L, 3 mmol/L, 5 mmol/L, 10 mmol/L, and 20 mmol/L; Sigma-Aldrich, St. Louis, MO, USA, 71945) and incubated for another 2 days. In experiments using BAPTA-AM (Sigma-Aldrich, A1076) to chelate intracellular Ca^{2+}, the explants were exposed to 10 μmol/L BAPTA-AM 15 min prior to incubation with salicylate. The timeline of the experimental process is shown in Fig. 1A.

Cochlear Immunofluorescence

For immunofluorescence, the basilar membrane of the cochlea was fixed in 4% paraformaldehyde for 1 h, permeabilized with 1% Triton X-100 for 30 min, and blocked with 10% donkey serum for 2 h at room temperature. The cochlear samples were then incubated overnight at 4°C with two primary antibodies, rabbit anti-myosin 7a (Proteus Biosciences, Ramona, CA, USA; 1:400) and goat anti-prestin (Santa Cruz, San Francisco, CA, USA; 1:200). The next day, after three washes in PBS, the samples were incubated with secondary fluorescent antibodies for 2 h, and then with DAPI (Sigma-Aldrich, D9542) for 5 min for nucleic acid staining. The sensory epithelia were cover-slipped and dried, and the middle turn was used for examination under a Zeiss confocal microscope (LSM 800).

Cell Counts

Hair cells with normal nuclei and stained with myosin 7a were recognized as surviving hair cells, among which myosin 7a/prestin double-labeled cells were OHCs and the others were IHCs. For hair cell quantification, we imaged the entire middle cochlea under a Zeiss microscope with a 40× lens and the immunopositive cells were quantified by ImageJ software. The numbers of IHCs and OHCs were counted every 100 μm along the middle turn of the cochlear explants. Three cochlear explants were used for cell counting in each group, and the average value was calculated.

Whole-Cell Patch Clamp Recordings

After culture, the cochleas were rinsed with ice-cooled PBS and then transferred to the microscope chamber. As shown in Fig. 1C, voltage-clamp recordings were performed in IHCs at their basolateral face through an EPC10/2 amplifier (HEKA Electronics, Lambrecht Pfalz, Germany), driven by Patchmaster (HEKA Electronics). Recording pipettes were pulled from borosilicate glass capillaries (BF150-86-10, Sutter Instrument, Novato, CA, USA) using a horizontal microelectrode puller (P-97, Sutter Instrument) and coated with dental wax. The pipettes had a typical resistance of 5–7 MΩ when filled with pipette solution

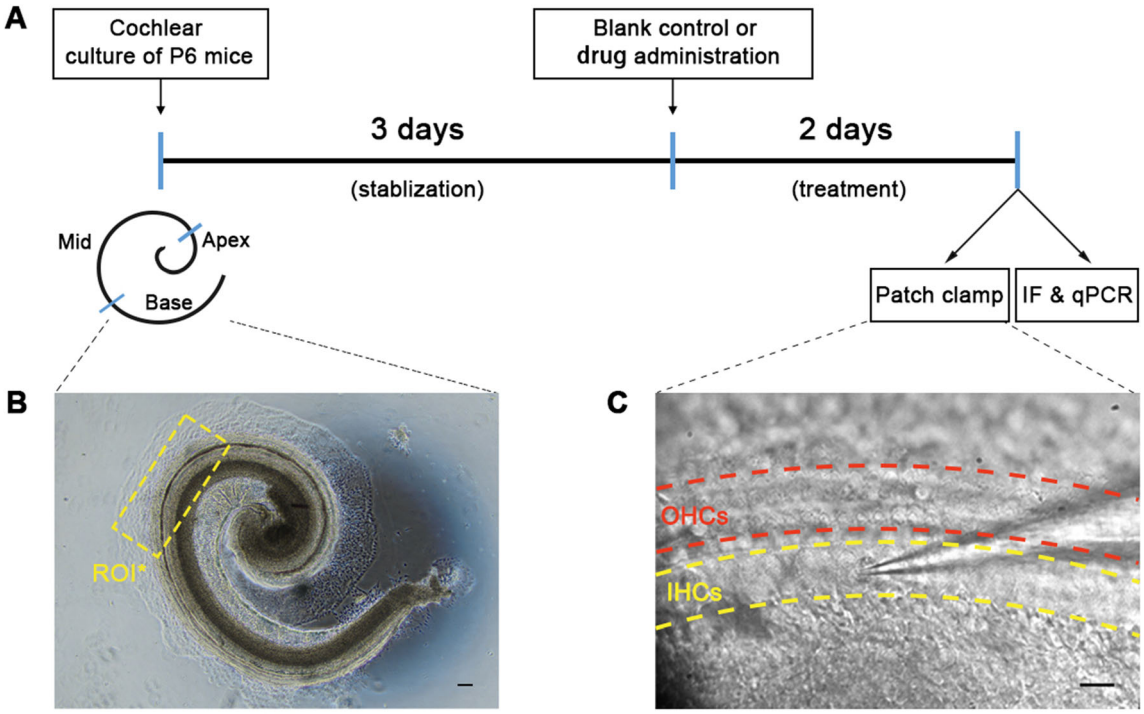

Fig. 1 Experimental design. **A** Timeline of the experimental protocol. P6, postnatal day 6; IF, immunofluorescence; qPCR, reverse transcription quantitative polymerase chain reaction. **B** Middle turn of a cochlear explant used for further experiments marked ROI (region of interest) (scale bar, 100 μm). **C** High magnification of a cochlea after 5 days in culture showing three rows of outer hair cells (OHCs), one row of inner hair cells (IHCs), and the approach to an inner hair cell with a recording pipette (40× water-immersion lens) (scale bar, 10 μm).

containing (in mmol/L) 135 Cs-methane sulfonate, 10 CsCl, 10 HEPES, 10 TEA-Cl, 2 EGTA (unless otherwise specified in the figure legend), 3 Mg-ATP, and 0.5 Na-GTP (290 mOsm, pH 7.20). The standard extracellular solution contained the following (in mmol/L): 125 NaCl, 2.8 KCl, 5 $CaCl_2$, 1 $MgCl_2$, 10 HEPES, 2 Na-pyruvate, and 5.6 D-glucose (295 mOsm, pH 7.40). When recording Ca^{2+} tail currents, we included the Ca^{2+} channel agonist (±)-BayK8644 (5 μmol/L; Sigma-Aldrich, B112) in the extracellular solution. (±)-BayK8644 increases the Ca^{2+} influx at voltage-gated Ca^{2+} channels, enabling faithful assessment of the whole-cell recordings [20, 21]. All patch-clamp experiments were carried out at room temperature (20°C–25°C) and the liquid junction potential was corrected offline.

IHCs were generally held at − 90 mV. The conductance–voltage relationship was determined from the Ca^{2+} current response to ramp stimulation from − 90 mV to + 50 mV, and was then used to calculate the peak amplitude (I_{Ca}), half-activation voltage (V_{half}), and slope factor (k_{slope}) as described previously [22]. Whole-cell membrane capacitance (C_m) was measured using a lock-in feature and the "Sine + DC" method [22]. The net increase of C_m after stimulation (ΔC_m) was used to assess the total synaptic vesicle exocytosis from IHCs. Noise analysis of Ca^{2+} tail currents was used to estimate the total number of Ca^{2+} channels and their single-channel current [23]. For each hair cell, after 100 consecutive Ca^{2+} current recordings, the mean (I_{mean}) and variance (var) of these currents were calculated using a custom-made program in Igor Pro (WaveMetrics, Lake Oswego, OR, USA). The data were fitted to a parabolic function according to the equation $var = i_{Ca} \cdot I_{mean} - I_{mean}^2/N_{Ca} + E_{noise}$, where i_{Ca} is the single-channel current, N_{Ca} is the number of Ca^{2+} channels per IHC, and E_{noise} is the electrical noise (5.57 ± 2.35 pA in the present study).

Reverse Transcription Quantitative Polymerase Chain Reaction (RT-qPCR)

After incubation, the middle turn of the basilar membrane was placed in TRIzol reagent (Ambion, Carlsbad, CA, USA). Total mRNA was extracted using the manufacturer's protocol and then reverse-transcribed into the cDNA using PrimeScript™ II 1st Strand cDNA Synthesis Kit (Takara Bio, Dalian, China). Quantitative real-time PCR was performed using TB Green Premix Ex Taq II (Takara Bio) on a 7500 Real Time PCR System (Applied Biosystems, CA, USA). The reaction mixture (20 μL) was as follows: 10 μL TB Green Premix Ex Taq II, 1 μL forward

primer (10 μmol/L), 1 μL reverse primer (10 μmol/L), 0.4 μL ROX Reference Dye II, 2 μL cDNA template, and 5.6 μL RNase-free ddH_2O. The PCR amplification procedure included two stages: pre-denaturation at 95°C for 30 s, and then 40 cycles of denaturation at 95°C for 5 s, and annealing and extension at 60°C for 34 s. The primer sequences of $Ca_V1.3$ were: 5′-GCTTACGTTAGGAATG-GATGGAA-3′ forward and 5′-GAAGTGGTCTTAA-CACTCGGAAG-3′ reverse. Relative mRNA transcript abundance was calculated by the standard curve method and standardized by the corresponding quantity of the housekeeping gene GAPDH (forward: 5′-TGGCCTTCCGTGTTCCTAC-3′, reverse: 5′-TGGCCTTCCGTGTTCCTAC-3′). Experiments in each group were repeated three times in an independent manner.

Data Analysis and Statistical Tests

The patch clamp measurements were estimated and analyzed in Igor Pro (WaveMetrics) with home-made macros. The statistical tests were performed in SPSS Statistics v.25 (IBM Corp, Armonk, NY, USA) with built-in functions. On the basis of the features of the data set, statistical significance was evaluated with unpaired Student's *t*-test or one-way ANOVA followed by the Least Significant Difference test. Data are presented as the mean ± SD in the text and as the mean ± SEM in the figures. The level of significance was defined as $P < 0.05$.

Results

IHCs are More Susceptible to Salicylate Damage than OHCs

The typical status of cochlear hair cells in control medium and cultures treated with 1 mmol/L, 3 mmol/L, 5 mmol/L, 10 mmol/L, or 20 mmol/L of salicylate for 48 h is shown in Fig. 2A. Three rows of OHCs and one row of IHCs grew well and maintained their normal locations in the control group. Treatment with 1 mmol/L–5 mmol/L salicylate had no noticeable effect on hair cell survival or morphology. After 2 days of treatment with 10 mmol/L salicylate, although OHCs remained intact, IHCs were dramatically damaged, showing markedly swollen, disrupted, or shrunken morphology. At 20 mmol/L, salicylate destroyed both IHCs and OHCs. Besides hair cell loss, the remaining hair cells showed significant chromatin condensation and cell shrinkage. To quantitatively determine the degree of cochlear hair cell damage, we counted the living IHCs and OHCs in each treatment group. The results showed that the number of IHCs was significantly lower in the 10 mmol/L and 20 mmol/L salicylate groups than in the other four groups (Fig. 2B). Although the 20 mmol/L salicylate group showed evident OHC death, the number of OHCs per 100 μm did not significantly differ from the other groups (one-way ANOVA, $F = 1.547$, $P = 0.248$, Fig. 2C). The main reason for this might be that the severe cell shrinkage resulted in decreased cell volume, which negated the impact of OHC loss and kept the number of OHCs per 100 μm intact. Given the severe IHC damage after 10 mmol/L or 20 mmol/L salicylate treatment, the subsequent experiments were only conducted at concentrations ranging from 0 mmol/L to 5 mmol/L.

Salicylate Increases the Ca^{2+} Current in IHCs in a Dose-dependent Manner

We made whole-cell patch-clamp recordings in IHCs from the middle turn of cochlear explants. First, ramp stimulation was applied to record the Ca^{2+} current (I_{Ca}; Fig. 3A). We found that salicylate treatment induced a larger peak amplitude of I_{Ca} in a dose-dependent manner (Fig. 3B). The average I_{Ca} was − 255 ± 52.0 pA, − 253 ± 67.1 pA, − 329 ± 66.7 pA, and − 447 ± 40.3 pA after 0 mmol/L, 1 mmol/L, 3 mmol/L, and 5 mmol/L salicylate treatment, respectively. Next, to characterize the functional status of IHCs more comprehensively, the V_{half} and k_{slope} were calculated to define the steepness of voltage dependence in Ca^{2+} current activation. We found that Ca^{2+} current had a more negative V_{half} after 3 mmol/L and 5 mmol/L salicylate treatment (Fig. 3C), and a steeper k_{slope} after 5 mmol/L salicylate treatment (Fig. 3D), suggesting that Ca^{2+} channels in IHCs had a higher Ca^{2+} sensitivity after salicylate treatment. In detail, after 0 mmol/L, 1 mmol/L, 3 mmol/L, and 5 mmol/L salicylate treatment, the average V_{half} was − 29.2 ± 3.14 mV, − 29.7 ± 3.39 mV, − 32.4 ± 2.65 mV, and − 33.5 ± 2.41 mV and the average k_{slope} was 5.05 ± 0.971 mV, 5.26 ± 0.890 mV, 4.60 ± 0.962 mV, and 4.06 ± 0.948 mV, respectively.

Salicylate Does Not Affect Exocytosis of IHCs, but Decreases the Efficiency of Ca^{2+} in Triggering Exocytosis

To assess exocytosis in IHCs after salicylate treatment, we applied step stimulation and measured the capacitance increase (ΔC_m, Fig. 4A), which can be used to assess the surface area change and synaptic vesicle release of IHCs. We varied the stimulus duration from 20 ms to 200 ms and found more Ca^{2+} influx (Q_{Ca}) in IHCs after salicylate treatment under varying conditions (Table 1 and Fig. 4B), consistent with the above finding that Ca^{2+} current had a larger peak amplitude after salicylate treatment. Multiple comparisons showed that Q_{Ca} increased significantly after 5 mmol/L salicylate treatment compared with the three

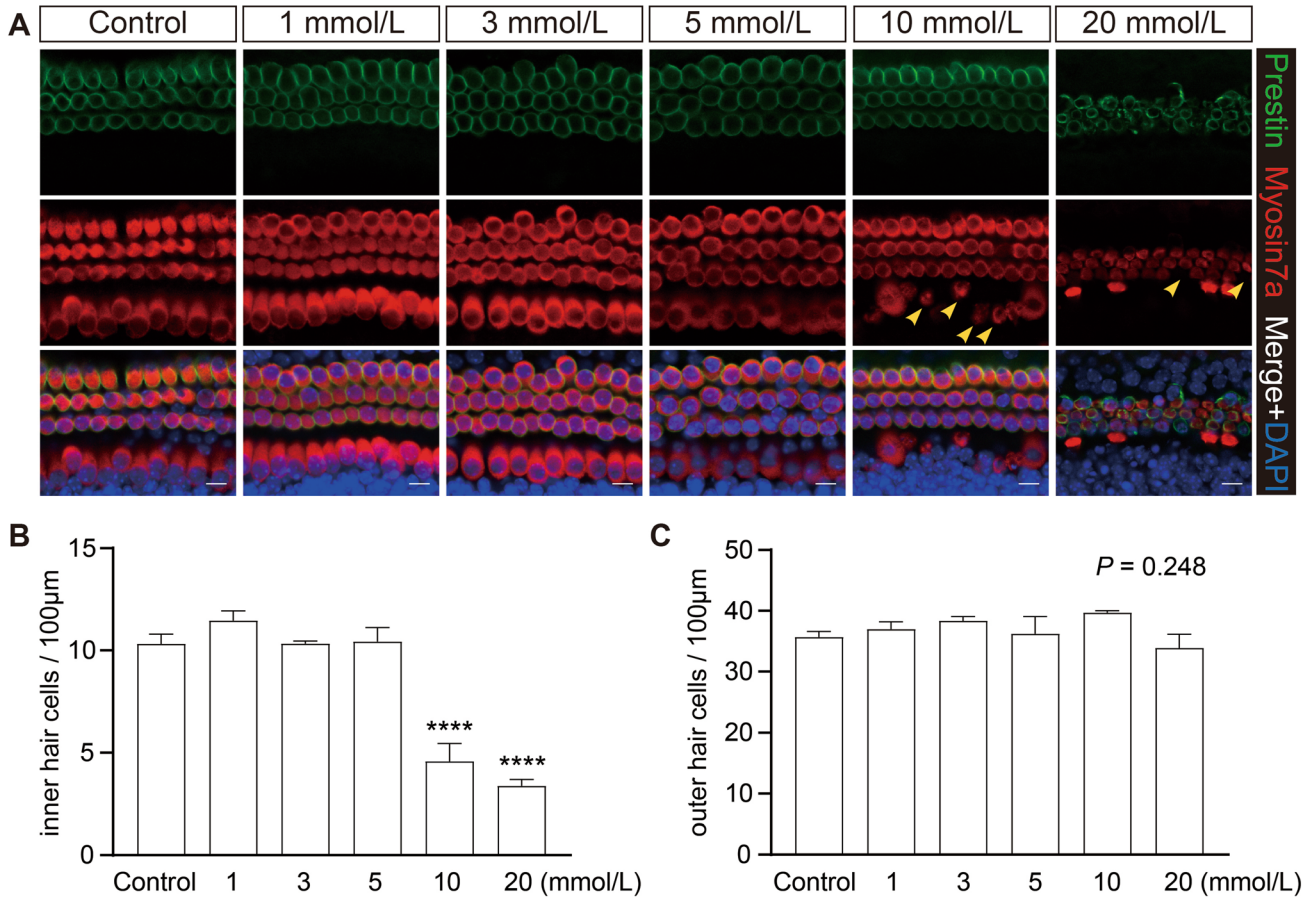

Fig. 2 Morphological changes of cochlear hair cells induced by different concentrations of salicylate. **A** Representative images of immunofluorescence staining for prestin (green), myosin 7a (red), and DAPI (blue) in the middle turn of the cochlea in different groups (arrowheads, damaged inner or outer hair cells; scale bars, 10 μm). **B** Quantification of inner hair cells from different groups (****P <0.0001 *vs* control, 1, 3, and 5 mmol/L salicylate group, one-way ANOVA). **C** Numbers of outer hair cells per 100 μm show no significant difference among the six groups. Data are presented as the mean ± SEM; n = 3 cochlear explants per group; statistical significance by one-way ANOVA followed by the Least Significant Difference test.

other groups (all P <0.01, least significant difference). Although Ca^{2+} entry provides the necessary trigger for exocytosis, no significant difference in ΔC_m was found among the four groups (Table 1 and Fig. 4C). One might argue that the lack of enhanced exocytosis was attributable to a relatively high concentration of intracellular EGTA (2 mmol/L). However, we showed here that decreasing the intracellular EGTA concentration (0.2 mmol/L) did not change the exocytosis in IHCs (Fig. 4D). We conclude that salicylate has little effect on vesicle release from IHCs.

Because of the increased Q_{Ca} and unchanged ΔC_m, the resulting efficiency of Ca^{2+} in triggering exocytosis, i.e., the $\Delta C_m/Q_{Ca}$ ratio, was significantly decreased in the 3mmol/L and 5 mmol/L salicylate treatment groups compared with the control group (Table 1). Furthermore, the decrease of $\Delta C_m/Q_{Ca}$ ratio was found for stimuli of 20 ms, 50 ms, and 100 ms (Table 1 and Fig. 4E–G), suggesting that salicylate affects the efficiency of Ca^{2+} in triggering exocytosis for both relatively short (20 ms) and long (100 ms) stimuli.

Salicylate Enhances Ca^{2+} Current by Increasing the Number of L-type Ca^{2+} Channels and Up-regulating $Ca_V1.3$ Expression in IHCs

We estimated the total number of Ca^{2+} channels in each hair cell using non-stationary noise analysis of Ca^{2+} tail currents. The IHC was initially kept at − 90 mV, transiently hyperpolarized to − 100 mV to relieve the inactivation of any steady-state, and then depolarized to + 40 mV for 10 ms to turn on all Ca^{2+} channels (Fig. 5A). We also included (±)-BayK8644, an L-type Ca^{2+} channel agonist, in the extracellular solution to maximize the open probability of Ca^{2+} channels and stabilize the recordings. Fig. 5A shows representative Ca^{2+} tail currents evoked in IHCs after different salicylate treatments. An ensemble of 100 repeated current sweeps was analyzed as one

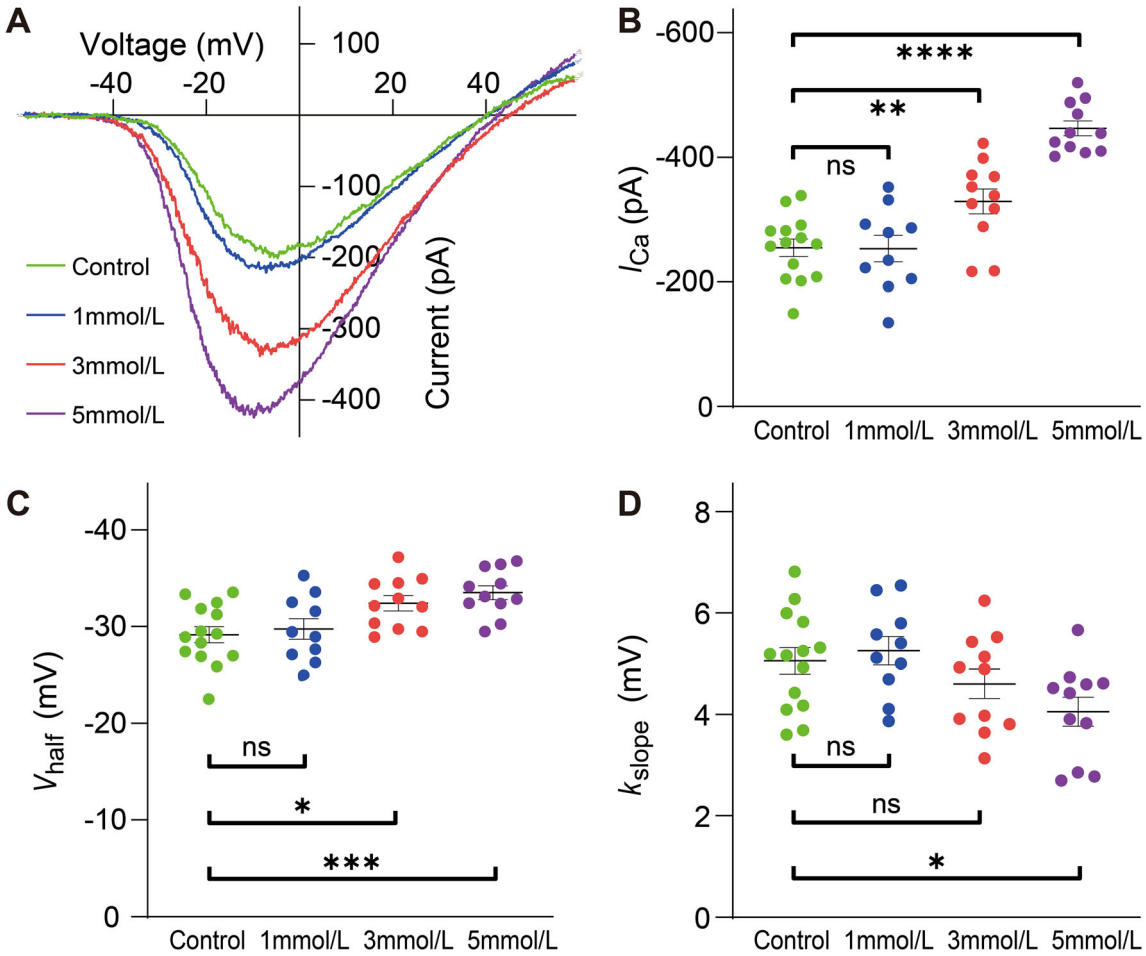

Fig. 3 Ca^{2+} current in inner hair cells (IHCs) after exposure to different concentrations of salicylate. **A** Representative Ca^{2+} currents recorded from four IHCs, one from each treatment group. **B** Peak amplitude (I_{Ca}) of Ca^{2+} current. **C** Half-activation voltage (V_{half}) of Ca^{2+} current. **D** Slope factor (k_{slope}) of Ca^{2+} current. Data are presented as the mean ± SEM. ns, P >0.05, *P <0.05, **P <0.01, ***P <0.001, ****P <0.0001, unpaired Student's t-test; n = 14, 10, 11, and 11 IHCs in control, 1, 3, and 5 mmol/L salicylate groups, respectively.

recording. By calculating and plotting the variance of the Ca^{2+} tail current against its mean (Fig. 5B, C), the total number of Ca^{2+} channels in one IHC (N_{Ca}) and their single-channel current (i_{Ca}) were estimated by fitting the data using a parabolic function (see Materials and Methods). Table 2 summarizes the findings from each IHC. The average i_{Ca} differed little among all four groups (one-way ANOVA, F = 0.823, P = 0.489, Fig. 5D). However, the number of Ca^{2+} channels in single IHCs increased remarkably after 3 or 5 mmol/L salicylate treatment (Fig. 5E), suggesting that changes in the number of Ca^{2+} channels might be the reason why IHCs have a larger peak amplitude of Ca^{2+} current after salicylate treatment.

As the main Ca^{2+} channel of immature mouse cochlear IHCs is the $Ca_V1.3$ type [24], we used RT-qPCR to determine its mRNA expression level. We found that the expression of $Ca_V1.3$ was significantly increased after 5 mmol/L salicylate treatment compared with the three other groups (Fig. 5F). Specifically, we found approximately 1.5-fold increases compared with the control and 1 mmol/L group, and a 1.3-fold increase compared with the 3 mmol/L group. The above results suggested that a transcription regulation mechanism might be involved in the electrophysiological change induced by salicylate treatment.

Inhibition of Ca^{2+} Overload Attenuates IHC Death Induced by Salicylate

Intracellular Ca^{2+} is a ubiquitous second messenger and Ca^{2+} overload is considered to be one of the most important mechanisms of cell injury. We used BAPTA-AM pretreatment to study the mechanism of the salicylate-induced electrophysiological and morphological changes in IHCs. Our data showed that pretreatment with BAPTA-AM, an intracellular Ca^{2+} chelator, protected IHCs from the cell death induced by 10 mmol/L salicylate (Fig. 6A,

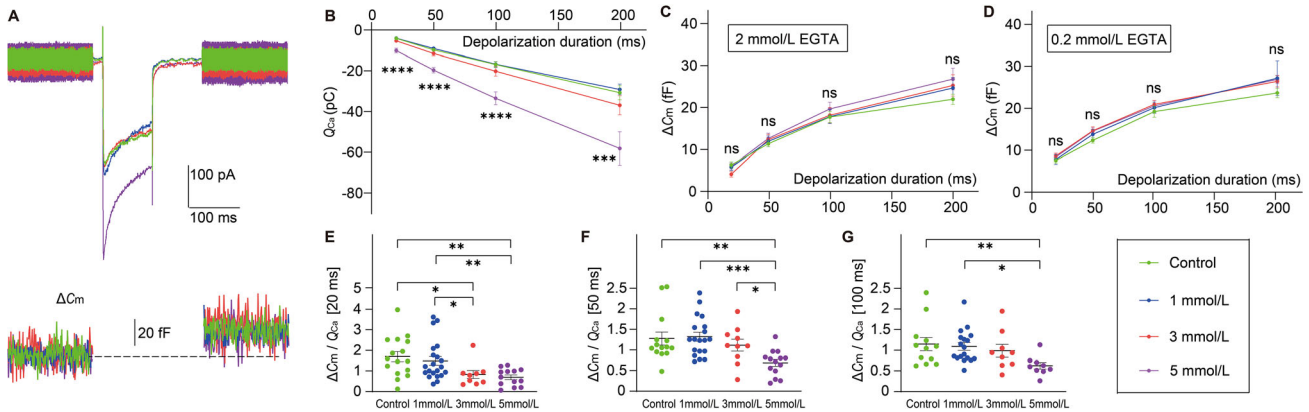

Fig. 4 Exocytosis from inner hair cells (IHCs) after exposure to different concentrations of salicylate. **A** Representative Ca^{2+} currents (upper panel) and exocytotic capacitance increase (ΔC_m, lower panel) in response to 100 ms depolarization recorded from four IHCs, one from each treatment group. **B** Ca^{2+} influx (Q_{Ca}) of IHCs in response to stimulation from 20 to 200 ms. **C** Capacitance change (ΔC_m) of IHCs with 2 mmol/L intracellular EGTA. **D** Capacitance change (ΔC_m) of IHCs with 0.2 mmol/L intracellular EGTA. **E–G** The efficiency of exocytosis, i.e., the $\Delta C_m/Q_{Ca}$ ratio, in response to stimulation for 20 ms **(E)**, 50 ms **(F)**, and 100 ms **(G)**. Data are presented as the mean ± SEM; ns $P > 0.05$, *$P < 0.05$, **$P < 0.01$, ***$P < 0.001$, ****$P < 0.0001$, one-way ANOVA **(B–D)** followed by Least Significant Difference test **(E–G)**.

Table 1 Summary of ΔC_m, Q_{Ca}, and $\Delta C_m/Q_{Ca}$ of inner hair cells in different groups for stimulation from 20 to 200 ms.

	Group	20 ms	50 ms	100 ms	200 ms
ΔC_m (fF)	Control	6.20 ± 3.04 (n = 16)	11.3 ± 2.76 (n = 14)	17.6 ± 4.68 (n = 12)	21.8 ± 3.67 (n = 9)
	1 mmol/L	5.68 ± 3.63 (n = 21)	11.8 ± 5.69 (n = 19)	17.7 ± 7.16 (n = 18)	24.5 ± 10.1 (n = 16)
	3 mmol/L	4.02 ± 2.08 (n = 9)	12.2 ± 4.02 (n = 10)	18.0 ± 5.46 (n = 9)	25.1 ± 7.17 (n = 8)
	5 mmol/L	5.91 ± 3.07 (n = 13)	12.5 ± 4.72 (n = 14)	19.5 ± 4.77 (n = 9)	26.6 ± 7.36 (n = 8)
	F	0.989	0.182	0.234	0.523
	P	0.405	0.908	0.872	0.669
Q_{Ca} (pC)	Control	–4.09 ± 1.23 (n = 16) ****	–9.68 ± 2.71 (n = 14) ****	–16.9 ± 5.06 (n = 12) ****	–30.8 ± 10.3 (n = 9) ***
	1 mmol/L	–4.00 ± 1.48 (n = 21) ****	–9.04 ± 3.04 (n = 19) ****	–16.8 ± 5.83 (n = 18) ****	–29.2 ± 10.6 (n = 16) ****
	3 mmol/L	–5.26 ± 1.59 (n = 9) ****	–11.5 ± 3.63 (n = 10) ****	–20.2 ± 7.26 (n = 9) ***	–37.0 ± 13.5(n = 8) **
	5 mmol/L	–10.1 ± 3.97 (n = 13)	–19.7 ± 5.14 (n = 14)	–33.6 ± 9.46 (n = 9)	–58.3 ± 23.4 (n = 8)
	F	23.4	26.1	14.2	8.19
	P	< 0.0001	< 0.0001	< 0.0001	< 0.001
ΔC_m / Q_{Ca}	Control	1.70 ± 0.974 (n = 16) **$^{\#}$	1.28 ± 0.592 (n = 14) **	1.15 ± 0.550 (n = 12) **	0.804 ± 0.388 (n = 9)
	1 mmol/L	1.49 ± 0.958 (n = 21) **$^{\#}$	1.32 ± 0.477 (n = 19) ***	1.09 ± 0.394 (n = 18) *	0.860 ± 0.276 (n = 16)
	3 mmol/L	0.830 ± 0.580 (n = 9)	1.12 ± 0.457 (n = 10) *	0.987 ± 0.468 (n = 9)	0.795 ± 0.505 (n = 8)
	5 mmol/L	0.694 ± 0.416 (n = 13)	0.687 ± 0.312 (n = 14)	0.625 ± 0.227 (n = 9)	0.500 ± 0.170 (n = 8)
	F	4.89	5.61	3.03	2.11
	P	0.004	0.002	0.039	0.115

ΔC_m, net increase in whole-cell capacitance after stimulation; Q_{Ca}, Ca^{2+} influx; $\Delta C_m/Q_{Ca}$, ratio of ΔC_m to Q_{Ca}. Data are presented as the mean ± SD, and n indicates the number of IHCs. *$P < 0.05$, **$P < 0.01$, ***$P < 0.001$, ****$P < 0.0001$ *versus* the 5 mmol/L group; $^{\#}P < 0.05$ *vs* the 3 mmol/L group; one-way ANOVA for comparison among multiple groups, F and P values presented in the table; Least Significant Difference test used for comparison between two groups.

B), indicating that Ca^{2+} serves as a critical mediator linking the electrophysiological and morphological changes in IHCs.

Moreover, we found that BAPTA-AM attenuated the salicylate-induced effects on the activation gating properties of Ca^{2+} channels, including V_{half} (Fig. 6C), k_{slope} (Fig. 6D), and I_{Ca} (Fig. 6E). However, BAPTA-AM pretreatment did not reverse the increase in the number of Ca^{2+} channels (Fig. 6F), or the up-regulation of $Ca_V1.3$ expression (Fig. 6G). These data suggest that free Ca^{2+} is

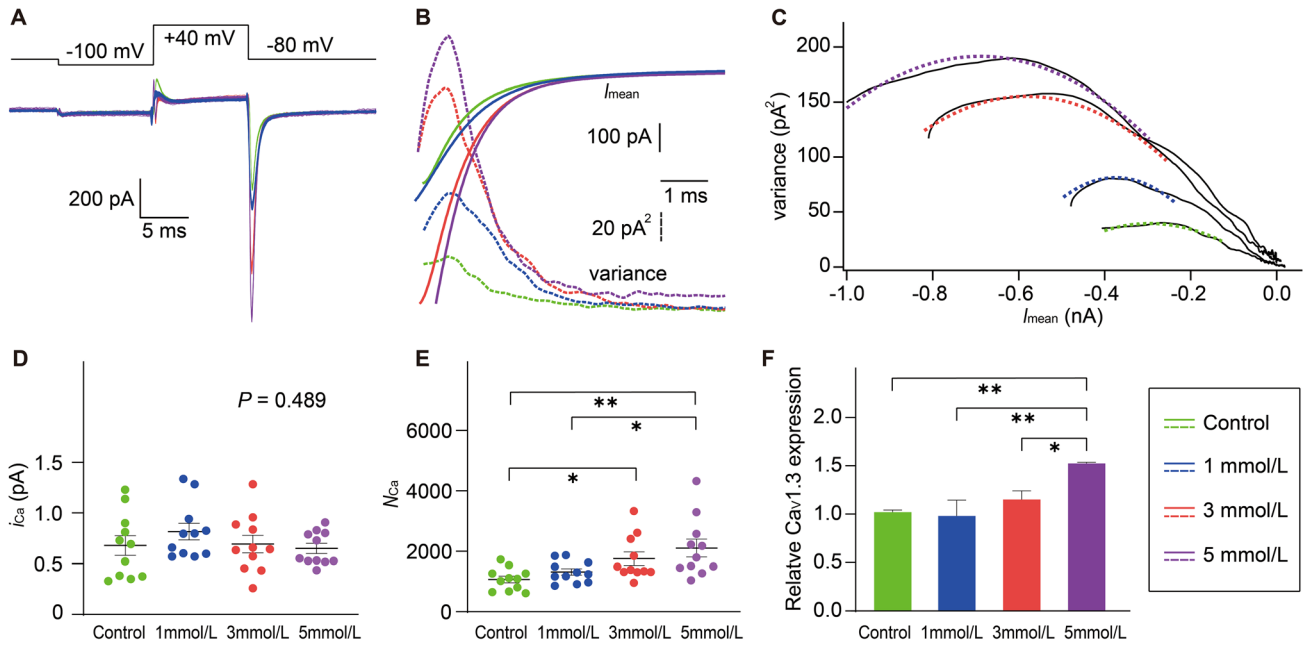

Fig. 5 Noise analysis of Ca^{2+} tail currents: the numbers of Ca^{2+} channels and single-channel current after exposure to different concentrations of salicylate. **A** The applied voltage clamp protocol (upper trace) and representative evoked Ca^{2+} tail currents (lower traces) recorded from four inner hair cells (IHCs), one from each treatment group. **B** The mean (I_{mean}, solid lines) and variance (dashed lines) calculated from the ensembles of Ca^{2+} tail currents as in **A**. **C** Variance plotted against the I_{mean} (solid lines) and fitted to a parabolic function (dashed lines). **D** The calculated single Ca^{2+} channel current (i_{Ca}) in IHCs does not significantly differ among the four groups (P = 0.489, one-way ANOVA). **E** Number of Ca^{2+} channels in single IHCs (N_{Ca}) (*P <0.05, **P <0.01, unpaired Student's t-test). **F** RT-qPCR determination of the mRNA expression of $Ca_V1.3$ reveals that $Ca_V1.3$ is up-regulated after salicylate treatment. Each experiment repeated three times. Data are presented as the mean ± SEM; *P <0.05, **P <0.01, Least Significant Difference test.

primarily involved in the direct effects of salicylate on Ca^{2+} channels, i.e., changes in voltage-dependence and Ca^{2+} current amplitude, but not the intracellular signaling pathways that may drive the up-regulation of $Ca_V1.3$ expression.

Discussion

To understand the role cochlear hair cells play in tinnitus generation, in this study, we investigated for the first time the IHC Ca^{2+} currents and exocytosis in salicylate-treated cochlear explants. We showed that salicylate did not affect synaptic vesicle exocytosis from IHCs. Instead, it had important influences on IHC Ca^{2+} currents, along with upregulation of the number of Ca^{2+} channels and the mRNA expression level of $Ca_V1.3$. The resulting Ca^{2+} overload became an important driving force for IHC death when exposed to high concentrations of salicylate. These findings may help to understand the neural mechanisms of salicylate-induced tinnitus.

Despite its high prevalence, most treatments are in lack of support of convincing clinical evidence [25], making it important to study the mechanisms underlying the induction of tinnitus. Presently, many studies indicate that cochlear hair cells play important roles in salicylate-induced tinnitus, but opinions differ. One view is that tinnitus develops as a result of active cochlear mechanics. Supporting evidence includes that chronic salicylate administration increases the expression of prestin (the OHC electromotility motor protein) and OHC electromotility [26, 27], consistent with the finding that the distortion product optoacoustic emission amplitudes are enhanced after similar salicylate treatment in guinea pigs [28]. Moreover, Zhang *et al.* reported specific upregulation of vesicular glutamate transporter 3 expression in cochlear IHCs in the rat model of tinnitus [29]. This molecule is responsible for transporting the neurotransmitter into secretory vesicles before synaptic transmission [30]. All these findings suggest a mechanism by which salicylate may induce tinnitus at the hair cell level. However, in the present study, we found that salicylate did not cause excessive exocytosis despite more Ca^{2+} influx into the IHCs. One possible reason is that the added Ca^{2+} channels in IHCs are nowhere near the vesicle release sites, which may leave the efficiency of Ca^{2+}-dependent exocytosis unaffected. Our data indicate that cochlear hair cells are not

Table 2 Noise analysis of inner hair cell Ca^{2+} tail currents.

Cell	Control		1 mmol/L		3 mmol/L		5 mmol/L	
	N_{Ca} (n)	i_{Ca} (n)	N_{Ca} (n)	i_{Ca} (n)	N_{Ca} (n)	i_{Ca} (n)	N_{Ca} (n)	i_{Ca} (n)
1	1265 ± 74 (2)	0.73 ± 0.05 (2)	972 ± 115 (3)	1.33 ± 0.52 (3)	1316 ± 263 (5)	0.84 ± 0.11 (5)	2221 ± 27 (3)	0.53 ± 0.17 (3)
2	649 ± 89 (2)	1.14 ± 0.10 (2)	1846 ± 65 (3)	0.57 ± 0.23 (3)	3337 ± 193 (2)	0.58 ± 0.19 (2)	4331 ± 192 (2)	0.44 ± 0.07 (2)
3	670 (1)	0.38 (1)	1173 ± 40 (2)	0.80 ± 0.09 (2)	1306 ± 162 (2)	1.00 ± 0.06 (2)	1509 ± 6 (2)	0.52 ± 0.04 (2)
4	1115 ± 177 (2)	0.36 ± 0.08 (2)	913 ± 67 (3)	0.94 ± 0.21 (3)	2615 ± 185 (4)	0.44 ± 0.05 (4)	1454 ± 43 (2)	0.79 ± 0.26 (2)
5	1542 ± 47 (2)	0.39 ± 0.03 (2)	1870 ± 35 (2)	1.28 ± 0.88 (2)	960 ± 33 (2)	0.89 ± 0.09 (2)	1036 ± 64 (2)	0.91 ± 0.21 (2)
6	1732 ± 5 (2)	0.34 ± 0.01 (2)	1299 ± 68 (2)	0.61 ± 0.04 (2)	1850 ± 97 (2)	0.65 ± 0.23 (2)	2578 ± 165 (2)	0.73 ± 0.37 (2)
7	8085 ± 90 (2)	0.81 ± 0.11 (2)	1169 ± 130 (2)	0.83 ± 0.08 (2)	1314 ± 251 (2)	0.66 ± 0.04 (2)	1272 ± 271 (2)	0.83 ± 0.13 (2)
8	1091 ± 43 (2)	0.53 ± 0.07 (2)	862 ± 42 (3)	0.80 ± 0.07 (3)	1342 ± 251 (2)	1.28 ± 0.41 (2)	1496 ± 95 (2)	0.53 ± 0.09 (2)
9	611 ± 88 (2)	1.23 ± 0.20 (2)	1635 ± 194 (2)	0.60 ± 0.08 (2)	1487 ± 241 (3)	0.64 ± 0.02 (3)	3297 ± 211 (3)	0.80 ± 0.22 (3)
10	1262 ± 115 (2)	0.90 ± 0.03 (2)	1491 ± 7 (2)	0.66 ± 0.09 (2)	2409 ± 61 (2)	0.27 ± 0.15 (2)	1800 ± 45 (2)	0.54 ± 0.05 (2)
11	1019 ± 96 (4)	0.70 ± 0.09 (4)	1243 ± 113 (5)	0.57 ± 0.11 (5)	1385 ± 272 (4)	0.46 ± 0.18 (4)	2180 ± 110 (2)	0.56 ± 0.14 (2)
All	1069 ± 368 (11)	0.68 ± 0.32 (11)	1316 ± 354 (11)	0.82 ± 0.27 (11)	1756 ± 727 (11)	0.69 ± 0.28 (11)	2106 ± 985 (11)	0.65 ± 0.16 (11)

Non-stationary noise analysis of Ca^{2+} tail currents was used to estimate the total number of Ca^{2+} channels (N_{Ca}) in each inner hair cell and the single channel current (i_{Ca}) after different salicylate treatment. Data are presented as the mean ± SD, and n indicates the number of repeated measurements in one IHC.

involved in tinnitus generation by enhancing their neuronal input.

Another view is that the role cochlear hair cells play in tinnitus is as a trigger rather than a generator, while hyperactivity in the central auditory pathway constitutes the initial tinnitus signal [31]. A compelling fact is that hearing loss, especially when due to aging or acoustic insult, is the biggest risk factor and the most common comorbidity of tinnitus in humans [32]. Many studies suggest that decreased afferent input due to a peripheral lesion may lead to a compensatory down-regulation of inhibitory amino-acid neurotransmission, resulting in pathological neural activity in the central auditory pathway that underpins tinnitus [33]. In line with this hypothesis, different forms of salicylate-induced lesion have been reported in the auditory periphery, including shrinkage of spiral ganglion neurons and loss of their peripheral fibers [34, 35], loss of IHC ribbon synapses [36, 37], and mismatch between pre- and post-ribbon synapses [36]. In the present study, we found that IHCs were dramatically damaged after 10 mmol/L and 20 mmol/L salicylate treatment. Given the significantly enhanced Ca^{2+} influx, we supposed that excessive loading of Ca^{2+} may be the underlying cause of IHC death after high-dose salicylate treatment; this provides a possible molecular mechanism for the generation of hearing loss and subsequent tinnitus.

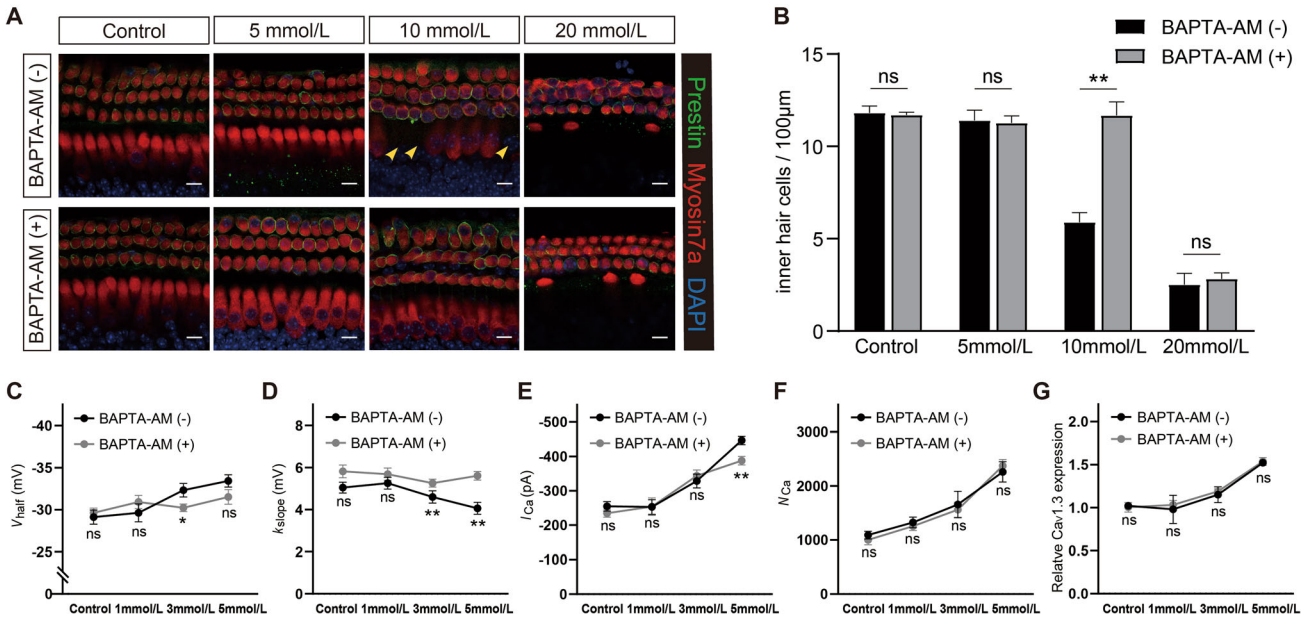

Fig. 6 Effects of BAPTA-AM on salicylate-exposed inner hair cells (IHCs). **A** Immunofluorescence staining for prestin (green), myosin 7a (red), and DAPI (blue) in the middle turn of the cochlea in different groups (arrowheads, damaged IHCs; scale bar, 10 μm). **B** Quantification of IHCs from different groups. **C–E** Half-activation voltage (V_{half}, **C**), slope factor (k_{slope}, **D**), and peak amplitude (I_{Ca}, **E**) of Ca^{2+} current in IHCs with or without BAPTA-AM pretreatment. **F** Numbers of Ca^{2+} channels (N_{Ca}) in IHCs with or without BAPTA-AM pretreatment. **G** RT-qPCR determination of the mRNA expression of $Ca_V1.3$ with or without BAPTA-AM pretreatment. Data are presented as the mean ± SEM. NS, $P > 0.05$, $^*P < 0.05$, $^{**}P < 0.01$, unpaired Student's *t*-test.

It is well documented that long-term Ca^{2+} overload damages IHCs by making them more vulnerable to Ca^{2+}-induced cytotoxicity [38]. In this study, we found that pretreatment with BAPTA-AM protected IHCs from cell death induced by 10 mmol/L salicylate, which is consistent with our speculation. However, BAPTA-AM did not protect IHCs from 20 mmol/L salicylate exposure, indicating that other mechanisms may also take part in salicylate-induced IHC death. For example, Xu *et al.* found that L-type Ca^{2+} channels are also involved in iron transport and iron-induced neurotoxicity [39].

It should be noted that the toxic effects of salicylate on cochlear spiral ganglion neurons are markedly stronger than on hair cells. Spiral ganglion neurons show significant soma shrinkage and nuclear condensation after 3 mmol/L salicylate exposure for 48 h when hair cells still have normal morphology [40]. Therefore, we cannot rule out the possibility that the electrophysiological changes we recorded in IHCs after 3 mmol/L or 5 mmol/L salicylate exposure were influenced indirectly by neuronal injury.

In addition, we explored possible reasons for more Ca^{2+} influx in salicylate-treated IHCs. On the one hand, salicylate caused a hyperpolarizing shift and steeper voltage-dependence in Ca^{2+} current activation, associated with a significantly decreased V_{half} and a steeper k_{slope}. These data suggest a role for salicylate in directly regulating $Ca_V1.3$ channel gating, which may act synergistically to cause considerably more Ca^{2+} influx into IHCs.

On the other hand, we investigated the number of L-type Ca^{2+} channels in each IHC. Using non-stationary fluctuation analysis of Ca^{2+} tail currents, we estimated that a single middle IHC in the P6 mouse cochlea contained 1069 Ca^{2+} channels. After 3 mmol/L or 5 mmol/L salicylate treatment, the channel count reached 1756 or 2106, which was equivalent to or even more than the channel count in the P13–P20 mouse cochlea (1711 in apical IHCs [20]). Combined with the increased $Ca_V1.3$ mRNA level, we supposed that salicylate enhances IHC Ca^{2+} influx by upregulating $Ca_V1.3$ expression. Interestingly, whole-cell patch clamp recordings of rat medial geniculate body slices have shown that salicylate (1.4 mmol/L) has no effect on the Ca^{2+} current mediated by T-type Ca^{2+} channels [41]. Unlike conventional synapses, IHC exocytosis is mainly mediated by Ca^{2+} influx through $Ca_V1.3$ L-type Ca^{2+} channel [19]. The Ca^{2+} channel type-specificity might be a factor causing the difference in mechanisms between peripheral and central auditory pathways in salicylate-induced tinnitus. Further studies are required to determine the specific Ca^{2+} channel type targeted by salicylate. Moreover, we found that attenuation of intracellular Ca^{2+} using BAPTA-AM did not affect the up-regulation of $Ca_V1.3$ expression, which did not support Ca^{2+}-dependent feed-forward signaling during salicylate treatment. Further

studies are needed to explore the intracellular signal mechanisms involved in the up-regulation of $Ca_V1.3$ expression after salicylate treatment.

The limitations of this study include the following two aspects. First, the cochlear explants were treated with a relatively large dose of salicylate for a very short time (48 h). However, in clinical practice, people with salicylate-induced tinnitus, such as patients with stroke [42] or cardiovascular diseases [43], usually take aspirin in low doses over the long term. Jastreboff *et al.* found that the maximum level of salicylate in perilymph was no more than 3 mmol/L following intraperitoneal injection of 460 mg/kg salicylate in rats [44]. Therefore, although a salicylate concentration gradient from 1 mmol/L to 5 mmol/L has frequently been used in *in vitro* studies [14, 34], we are of the opinion that the results of related studies need to be interpreted in caution. Especially extension of the morphological changes we found after 10 mmol/L or 20 mmol/L salicylate exposure to the mechanism of tinnitus generation should be treated with caution. Secondly, due to the limitations of the cochlear *in vitro* culture technique, we used mice on P6, when both Ca^{2+} current density (peak I_{Ca} normalized to the cell capacitance) and ΔC_m are maximal compared with other ages [45]. Cochlear samples at P6 are more sensitive and reflect any small changes in Ca^{2+} currents and exocytosis, but may also exaggerate the effect of salicylate on IHCs. Further experiments using mice at an older age, especially after the onset of hearing, will help to validate our findings. Nonetheless, for the first time, we performed whole-cell patch clamp on salicylate-treated cochleas from semi-intact organs of Corti, and provide a better understanding of the mechanisms of tinnitus.

In summary, our findings demonstrate that salicylate-induced tinnitus does not involve excessive exocytosis in cochlear IHCs. Instead, Ca^{2+} influx is significantly increased in IHCs with both the direct effects of salicylate on Ca^{2+} channel gating and the upregulation of $Ca_V1.3$ expression. Consequently, intracellular Ca^{2+} overload can cause IHC death, which may then become a trigger for tinnitus generation.

Acknowledgements We would like to express our gratitude to Mr. Yijiao Chen (Department of General Surgery, Zhongshan Hospital, Fudan University) for his help with data analysis. This work was supported by the National Natural Science Foundation of China (81770999 and 81670281), the Shanghai Municipal Commission of Science and Technology Research Project (18140900304, and 19140900902), and the Big Data and Artificial Intelligence Project (2020DSJ07).

Conflict of interest The authors declare that they have no conflict of interest.

References

1. Cazals Y. Auditory sensori-neural alterations induced by salicylate. Prog Neurobiol 2000, 62: 583–631.
2. Liu P, Qin D, Huang X, Chen H, Ye W, Lin X. Neurotoxicity of sodium salicylate to the spiral ganglion neurons: $GABA_A$ receptor regulates NMDA receptor by Fyn-dependent phosphorylation. J Comp Physiol A Neuroethol Sens Neural Behav Physiol 2019, 205: 469–479.
3. Liu Y, Zhang H, Li X, Wang Y, Lu H, Qi X, *et al*. Inhibition of voltage-gated channel currents in rat auditory cortex neurons by salicylate. Neuropharmacology 2007, 53: 870–880.
4. Qin DX, Liu PQ, Chen HY, Huang X, Ye WH, Lin XY, *et al*. Salicylate-induced ototoxicity of spiral ganglion neurons: Ca^{2+}/CaMKII-mediated interaction between NMDA receptor and $GABA_A$ receptor. Neurotox Res 2019, 35: 838–847.
5. Zugaib J, Ceballos CC, Leão RM. High doses of salicylate reduces glycinergic inhibition in the dorsal cochlear nucleus of the rat. Hear Res 2016, 332: 188–198.
6. Baguley D, McFerran D, Hall D. Tinnitus. Lancet 2013, 382: 1600–1607.
7. Bhatt JM, Bhattacharyya N, Lin HW. Relationships between tinnitus and the prevalence of anxiety and depression. Laryngoscope 2017, 127: 466–469.
8. McCormack A, Edmondson-Jones M, Somerset S, Hall D. A systematic review of the reporting of tinnitus prevalence and severity. Hear Res 2016, 337: 70–79.
9. Wang HT, Luo B, Zhou KQ, Xu TL, Chen L. Sodium salicylate reduces inhibitory postsynaptic currents in neurons of rat auditory cortex. Hear Res 2006, 215: 77–83.
10. Wang HT, Luo B, Huang YN, Zhou KQ, Chen L. Sodium salicylate suppresses serotonin-induced enhancement of GABAergic spontaneous inhibitory postsynaptic currents in rat inferior colliculus *in vitro*. Hear Res 2008, 236: 42–51.
11. Middleton JW, Kiritani T, Pedersen C, Turner JG, Shepherd GM, Tzounopoulos T. Mice with behavioral evidence of tinnitus exhibit dorsal cochlear nucleus hyperactivity because of decreased GABAergic inhibition. Proc Natl Acad Sci U S A 2011, 108: 7601–7606.
12. Guitton MJ, Caston J, Ruel J, Johnson RM, Pujol R, Puel JL. Salicylate induces tinnitus through activation of cochlear NMDA receptors. J Neurosci 2003, 23: 3944–3952.
13. Ruel J, Chabbert C, Nouvian R, Bendris R, Eybalin M, Leger CL, *et al*. Salicylate enables cochlear arachidonic-acid-sensitive NMDA receptor responses. J Neurosci 2008, 28: 7313–7323.
14. Kimitsuki T, Ohashi M, Umeno Y, Yoshida T, Komune N, Noda T, *et al*. Effect of salicylate on potassium currents in inner hair cells isolated from guinea-pig cochlea. Neurosci Lett 2011, 504: 28–31.
15. Wu T, Lv P, Kim HJ, Yamoah EN, Nuttall AL. Effect of salicylate on KCNQ4 of the guinea pig outer hair cell. J Neurophysiol 2010, 103: 1969–1977.
16. Kakehata S, Santos-Sacchi J. Effects of salicylate and lanthanides on outer hair cell motility and associated gating charge. J Neurosci 1996, 16: 4881–4889.
17. Fettiplace R, Hackney CM. The sensory and motor roles of auditory hair cells. Nat Rev Neurosci 2006, 7: 19–29.
18. Brandt A, Striessnig J, Moser T. CaV1.3 channels are essential for development and presynaptic activity of cochlear inner hair cells. J Neurosci 2003, 23: 10832–10840.
19. He YZ, Li W, Zheng ZW, Zhao LP, Li WY, Wang YF, *et al*. Inhibition of Protein arginine methyltransferase 6 reduces reactive oxygen species production and attenuates aminoglycoside- and cisplatin-induced hair cell death. Theranostics 2020, 10: 133–150.

20. Brandt A, Khimich D, Moser T. Few CaV1.3 channels regulate the exocytosis of a synaptic vesicle at the hair cell ribbon synapse. J Neurosci 2005, 25: 11577–11585.
21. Graydon CW, Cho S, Li GL, Kachar B, von Gersdorff H. Sharp Ca^{2+} nanodomains beneath the ribbon promote highly synchronous multivesicular release at hair cell synapses. J Neurosci 2011, 31: 16637–16650.
22. Liu HH, Li G, Lu JW, Gao YG, Song L, Li GL, *et al*. Cellular differences in the cochlea of CBA and B6 mice may underlie their difference in susceptibility to hearing loss. Front Cell Neurosci 2019, 13: 60.
23. Roberts WM, Jacobs RA, Hudspeth AJ. Colocalization of ion channels involved in frequency selectivity and synaptic transmission at presynaptic active zones of hair cells. J Neurosci 1990, 10: 3664–3684.
24. Platzer J, Engel J, Schrott-Fischer A, Stephan K, Bova S, Chen H, *et al*. Congenital deafness and sinoatrial node dysfunction in mice lacking class D L-type Ca^{2+} channels. Cell 2000, 102: 89–97.
25. Langguth B, Kreuzer PM, Kleinjung T, de Ridder D. Tinnitus: causes and clinical management. Lancet Neurol 2013, 12: 920–930.
26. Yang K, Huang ZW, Liu ZQ, Xiao BK, Peng JH. Long-term administration of salicylate enhances prestin expression in rat cochlea. Int J Audiol 2009, 48: 18–23.
27. Yu N, Zhu ML, Johnson B, Liu YP, Jones RO, Zhao HB. Prestin up-regulation in chronic salicylate (aspirin) administration: an implication of functional dependence of prestin expression. Cell Mol Life Sci 2008, 65: 2407–2418.
28. Huang ZW, Luo YY, Wu ZY, Tao ZZ, Jones RO, Zhao HB. Paradoxical enhancement of active cochlear mechanics in long-term administration of salicylate. J Neurophysiol 2005, 93: 2053–2061.
29. Zhang W, Peng Z, Yu S, Song QL, Qu TF, Liu K, *et al*. Exposure to sodium salicylate disrupts VGLUT3 expression in cochlear inner hair cells and contributes to tinnitus. Physiol Res 2020, 69: 181–190.
30. Takamori S, Malherbe P, Broger C, Jahn R. Molecular cloning and functional characterization of human vesicular glutamate transporter 3. EMBO Rep 2002, 3: 798–803.
31. Rauschecker JP, Leaver AM, Mühlau M. Tuning out the noise: Limbic-auditory interactions in tinnitus. Neuron 2010, 66: 819–826.
32. Miyakawa A, Wang WH, Cho SJ, Li DL, Yang S, Bao SW. Tinnitus correlates with downregulation of cortical glutamate decarboxylase 65 expression but not auditory cortical map reorganization. J Neurosci 2019, 39: 9989–10001.
33. Wang HN, Brozoski TJ, Caspary DM. Inhibitory neurotransmission in animal models of tinnitus: maladaptive plasticity. Hear Res 2011, 279: 111–117.
34. Wei L, Ding D, Salvi R. Salicylate-induced degeneration of cochlea spiral ganglion neurons-apoptosis signaling. Neuroscience 2010, 168: 288–299.
35. Zheng JL, Gao WQ. Differential damage to auditory neurons and hair cells by ototoxins and neuroprotection by specific neurotrophins in rat cochlear organotypic cultures. Eur J Neurosci 1996, 8: 1897–1905.
36. Cui WM, Wang HL, Cheng Y, Ma XR, Lei Y, Ruan XX, *et al*. Long-term treatment with salicylate enables NMDA receptors and impairs AMPA receptors in C57BL/6J mice inner hair cell ribbon synapse. Mol Med Rep 2019, 19: 51–58.
37. Zhang W, Peng Z, Yu SK, Song QL, Qu TF, He L, *et al*. Loss of cochlear ribbon synapse is a critical contributor to chronic salicylate sodium treatment-induced tinnitus without change hearing threshold. Neural Plast 2020, 2020: 3949161.
38. Orrenius S, Zhivotovsky B, Nicotera P. Regulation of cell death: the calcium-apoptosis link. Nat Rev Mol Cell Biol 2003, 4: 552–565.
39. Xu YY, Wan WP, Zhao S, Ma ZG. L-type calcium channels are involved in iron-induced neurotoxicity in primary cultured ventral mesencephalon neurons of rats. Neurosci Bull 2020, 36: 165–173.
40. Deng LL, Ding DL, Su JP, Manohar S, Salvi R. Salicylate selectively kills cochlear spiral ganglion neurons by paradoxically up-regulating superoxide. Neurotoxicol Res 2013, 24: 307–319.
41. Wang XX, Jin Y, Luo B, Sun JW, Zhang J, Wang M, *et al*. Sodium salicylate potentiates the GABAB-GIRK pathway to suppress rebound depolarization in neurons of the rat's medial geniculate body. Hear Res 2016, 332: 104–112.
42. García Rodríguez LA, Cea Soriano L, Hill C, Johansson S. Increased risk of stroke after discontinuation of acetylsalicylic acid: a UK primary care study. Neurology 2011, 76: 740–746.
43. Miedema MD, Huguelet J, Virani SS. Aspirin for the primary prevention of cardiovascular disease: in need of clarity. Curr Atheroscler Rep 2016, 18: 4.
44. Jastreboff PJ, Hansen R, Sasaki PG, Sasaki CT. Differential uptake of salicylate in serum, cerebrospinal fluid, and perilymph. Arch Otolaryngol Head Neck Surg 1986, 112: 1050–1053.
45. Beutner D, Moser T. The presynaptic function of mouse cochlear inner hair cells during development of hearing. J Neurosci 2001, 21: 4593–4599.